Dipole-Dipole Interaction Between A Fluorescent Dye and a Phosphorescent Dopant In Solid Thin Films: A Concentration and Excitation Intensity Study

G. Ramos-Ortiz, Y. Oki[*]*, B. Domercq, and B. Kippelen*
Optical Sciences Center, University of Arizona, Tucson, Arizona
[*]*Current address: Graduate School of Information Science and Electrical Engineering, Kyushu University, Fukoka, Japan*

Abstract

Here we report on the long-range dipole-dipole Förster energy transfer between the fluorescent dye 4,4'-*N,N'*-dicarbazole-biphenyl (CBP) and the phosphorescent organometallic complex *fac* tris(2-phenylpyridine) iridium(III) (Ir(ppy)$_3$). The study is carried out for both molecules dispersed in a polymer matrix forming a solid thin film. By studying the photoluminescence of these films with various concentrations of Ir(ppy)$_3$ (guest) and CBP (host) molecules at various optical excitation conditions and by comparing our experimental results with the predictions of a numerical model of the Förster transfer process, we determined the total efficiency of energy transfer and a Förster interaction radius of 3 nm for the pair CBP:Ir(ppy)$_3$ without having to use time-resolved techniques. From this result, we discuss the optimum dopant to guest ratios in solid films of the pair CBP:Ir(ppy)$_3$ for maximum energy transfer following optical excitation.

Introduction

In recent years, energy transfer has been successfully used in variety of emissive devices including light-emitting diodes[1-2] and organic solid-state lasers.[3] Energy transfer between host and guest molecules can occur through either coulombic interactions or by electron exchange.[4] The former is referred to as dipole-dipole or Förster-type energy transfer and is a long-range interaction. Energy transfer that involves exchange of electrons is referred to as Dexter transfer. In OLED's, high photoluminescence efficiency can be achieved from diluted guest molecules through a rapid energy transfer from a host molecule. Energy transfer is also used in OLED displays to achieve red, green and blue colors through internal color conversion[2] while in organic solid state lasers it is used to shift the emission to longer wavelengths where self-absorption from the matrix is reduced.[3]

In organic electroluminescent devices based on fluorescent small molecules or polymers, emission originates from the recombination of singlet excited states. Since injection of charge carriers in these devices leads to the formation of both singlet and triplet states, the overall electroluminescence quantum efficiency is always limited to the ratio of singlets and triplets that are formed. To alleviate this limitation, organic electroluminescence based on phosphorescence (emission from a triplet excited state) was proposed.[5-8] When phosphorescent molecules are used as dopants in OLEDs, both singlet and triplet states formed by the injection of carriers can potentially be harvested since: (i) singlet excited states formed in the host can create singlet excited states of the guest through Förster energy transfer; (ii) these singlet excited states together with those formed directly on the guest can be transformed into triplet excited states of the guest through intersystem crossing; (iii) triplet excited states formed on the host can transfer their energy by a Dexter process to triplet excited states of the guest. The most common phosphorescent dopants used in OLEDs are the red emitting 2,3,7,8,12,13,17,18-octaethylporphine platinum (PtOEP)[6] and the green emitting *fac* tris(2-phenylpyridine)iridium (Ir(ppy)$_3$).[8]

In this paper, we investigate Förster energy transfer between Ir(ppy)$_3$ as a guest in the host 4,4'-*N,N'*-dicarbazole-biphenyl (CBP) which has been used in efficient electrophosphorescent devices.[8] The structure of these molecules and their spectra are shown in Fig. 1. Large Förster radius is generally observed when the emission of the host and the absorption spectrum of the guest overlap strongly. In this study the efficiency of energy transfer is measured by means of photoluminescence studies performed on thin films with various concentrations of guest and host molecules at various optical excitation conditions. By comparing our experimental results with the predictions of a numerical model of the Förster transfer process, we estimate the total efficiency of energy transfer and the radius R_0 for the pair CBP:Ir(ppy)$_3$ without having to use time-resolved techniques. Note that our studies focus on the optical excitation of the system CBP:Ir(ppy)$_3$ which differ from other studies where the system is electrically excited.[9] The paper is organized as follows: experimental methods are described first and are followed by a description of the numerical model we used to describe Förster transfer. Then, by comparing our model predictions with the experimental results we estimate the Förster radius R_0. From this result, we discuss the optimum dopant to guest ratios in solid films of the pair CBP:Ir(ppy)$_3$ for maximum energy transfer following optical excitation.

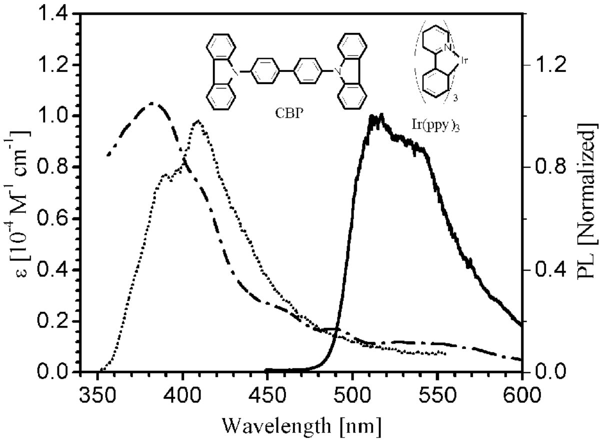

Figure 1. Photoluminescence spectrum (continuous curve) and absorption spectrum (dash-dotted curve) of Ir(ppy)$_3$ dispersed (5 wt %) in polystyrene. The emission spectrum of CBP (dotted curve) dispersed (5 wt %) in polystyrene.

Experimental Technique

Our thin films were prepared by spin-coating technique, processed from solutions of different concentration of CBP, Ir(ppy)$_3$ and as matrix polystyrene (PS) dissolved in chloroform. This composition PS:CBP:Ir(ppy)$_3$ was deposited on glass substrates. To study the photo-luminescence of host and guest molecules separately, we also prepared films with composition PS:CBP and PS:Ir(ppy)$_3$. The thickness of each film was measured by using a prism coupler (Metricon, model-2010) while their optical density were determined with the use of a spectrophotometer (Varian, model-Cary 5G). The samples were pumped by pulses of 150 fs at 310 nm with a repetition rate of rate of 1 kHz. This excitation was focused on the films in a spot with a radius of 40 µm. The emitted light from the films was collected by lenses and analyzed using a spectrometer.

Numerical Model of Förster Energy Transfer Efficiency in Optically Pumped Phosphorescent Thin Films

Various fluorescent organic molecules and polymers have been studied[10-14] under the approach of Förster energy transfer from donor (host) to an acceptor (guest). The rate k_{ET} of this transfer reaction can be written as:

$$k_{ET} = k\left(\frac{R_0}{R}\right)^6 \tag{1}$$

where k is the decay rate of the excited host molecules, R is the distance between the host that donates the energy and the guest to which the energy gets transferred and R_0 is the Förster radius. In this study we pursue to model the total energy transfer efficiency for given concentrations of guest and host molecules dispersed in a solid thin film. To do this, we start by writing the efficiency of energy transfer η_{ET}, for a single guest-host pair, that according to Eq. 1 is:

$$\eta_{ET} = \frac{k_{ET}}{k_{ET} + k} = \frac{1}{1 + (R/R_0)^6} \tag{2}$$

Here we point out that when the molecules are dispersed in an amorphous film η_{ET} is a function of R, the distance between interacting guest-host pairs. To calculate an average value of η_{ET} we divide the continuous parameter R in discrete distances R_j with an interval between R_j and R_{j+1} of 0.2 nm (with j = 1, 2, 3…and $R_{j=1}$ = 0). After this, we create a distribution function $g(R_j)$ that gives the probability to find an excited host molecule (H^*) at a distance R from a guest molecule (G) in the ground state, with $R_j < R < R_{j+1}$. Obviously, the magnitude of $g(R_j)$, for any given interval, depends on the density of guest molecules N_G and the available concentration of excited host molecules N_{H*} created in a film having a total host molecule density N_H. The density N_{H*} will vary along the depth of the film that is optically excited. This inhomogeneous excitation profile can be accounted for by dividing the thickness L of the film into M equal small segments, each one with a coordinate z_i ($1 \le i \le M$). Then, the density of excited host molecules at a given depth z_i can be written as:

$$N_{H*}(z_i, I_0) = \frac{I_0 \alpha_H}{\hbar\omega} \exp - \alpha_H z_i \tag{3}$$

where I_0 is the energy per laser pulse per unit area, α_H is the extinction coefficient of the film due to CBP absorption and $\hbar\omega$ is the photon energy. Since the distribution of distances between interacting molecules depends on the concentration of doping molecules and concentration of excited host molecules, we adopt the notation $g(R_j(N_G,N_{H*}(z_i,I_0)))$ for our distribution function. This function, in combination with Eq. 2, is used to evaluate the average energy transfer efficiency between a set of excited host molecules and guest molecules in the ground state localized at the depth position z_i in a thin film:

$$< \eta_{ET}(z_i, I_0) >_i = \Gamma \sum_{j=1}^{\infty} g(R_j(N_G, N_{H*}(z_i, I_0))) \times \eta_{ET} \tag{4}$$

Here, we introduce the parameter Γ to take into account the energy loss induced by uncoupled excited host molecules. For instance, in our study the excitation (pulses of 150 fs) is much shorter than the lifetime τ_H of the excited CBP (H^*) and the lifetime τ_G of the excited Ir(ppy)$_3$ (G^*). Since $\tau_H << \tau_G$, at most only one excited state can be generated in each Ir(ppy)$_3$ molecule for each pumping pulse. Hence, when $N_{H^*} > N_G$, some of the excited states created in CBP will relax without transferring their energy to Ir(ppy)$_3$. In this case, we assume $\Gamma = N_G / N_{H^*}$. On the other hand, when $N_{H^*} \leq N_G$, every excited-state created in CBP finds a guest molecule in the ground state to couple with, leading to $\Gamma = 1$.

To calculate $g(R_j)$ at a given film depth z_i, we considered a large population (30,000) of excited host molecules and guest molecules dispersed randomly in a small cube of a given volume. This numerical simulation was made using a random function. To simulate various excited host and guest concentrations, we kept the population constant and varied the volume of the cube accordingly. Then, we used an algorithm to count the guest-host pairs within a given range R_j, assuming that an excited host molecule interacts only with its nearest guest. Figure 2 shows a distribution of the density of coupled guest-host pairs obtained numerically by this method for particular molecular densities N_H and N_G.

From the volume partition that we have considered in Eqs. (3-4), it derives that the total energy transfer efficiency in a film of thickness L is:

$$<\eta_{ET}(I_0)>=\frac{\sum_{i=1}^{M}<\eta_{ET}(z_i,I_0)>_i N_{H^*}(z_i,I_0)}{\sum_{i=1}^{M}N_{H^*}(z_i,I_0)} \tag{5}$$

Note that with our way of proceeding, the total energy transfer efficiency $<\eta_{ET}(I_0)>$ is defined as the ratio of the total number of excited Ir(ppy)$_3$ molecules (created through Förster transfer) and the total number of absorbed photons by CBP. Thus, the value of $<\eta_{ET}(I_0)>$, that we can evaluate by numerical methods, is related to the time integrated phosphorescence signal $PL_{PH}(I_0)$, that can be detected experimentally from a film of thickness L under excitation I_0, through:

$$PL_{PH}(I_0)=I_0(1-\exp-\alpha_H L)\chi\eta_{PL}(N_G)<\eta_{ET}(I_0)> \tag{6}$$

here χ is a constant of proportionality for the phosphorescence signal detected by our apparatus, while $\eta_{PL}(N_G)$ is the photoluminescence quantum yield of Ir(ppy)$_3$ when excited initially into a singlet excited state. For convenience, we express this quantum yield as:

$$\eta_{PL}(N_G)=Q(N_G)\eta_{PL}(N_{G0})\eta_{ISC} \tag{7}$$

where $\eta_{PL}(N_{G0})$ is the phosphorescence quantum yield of Ir(ppy)$_3$ at the low concentration N_{G0} while Q is a concentration quenching factor that accounts for the decrement of such quantum yield at higher concentrations ($Q \leq 1$ and $Q(N_{G0}) = 1$). In Eq. 6 we neglect the direct absorption of photons by Ir(ppy)$_3$ and also assumed that energy gets transferred from the singlet excited-state of the host to the singlet excited-state of the phosphor, which in turn gets transferred to the first triplet excited-state by intersystem crossing with efficiency η_{ISC}.

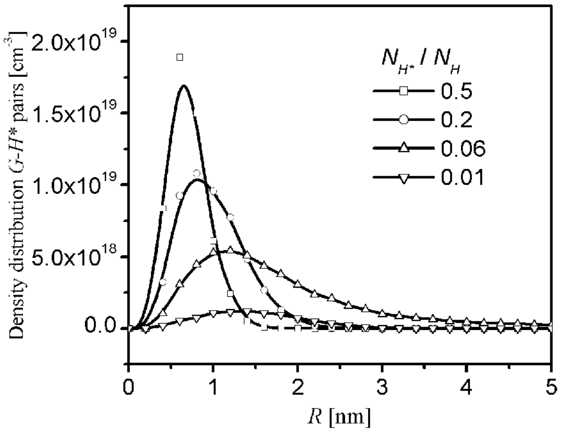

Figure 2. Density distribution of guest-host pairs calculated numerically for a small portion of film volume with densities N_H = 9.1×10^{20} cm^{-3} and N_G = 5.1×10^{19} cm^{-3} for various ratios of N_{H^*}/N_H. Lines are a guide to the eye.

Results and Discussion

Now proceed to compare our model predictions summarized in Eq. 5 with the experimental results calculated from Eq. 6. In latter equation, however, the term χ and the absolute value of $\eta_{PL}(N_G)$ are difficult to evaluate experimentally. For this reason we also measured the photoluminescence of films with compositions PS:Ir(ppy)$_3$ in the same geometry. These kinds of samples were used as reference. In such films, the phosphorescence emission denoted as $PL'_{PH}(I_0)$ is simply given by:

$$PL'_{PH}(I_0)=I_0(1-\exp-\alpha'_G L')\chi\eta_{PL}(N'_G) \tag{8}$$

where α'_G is the absorption coefficient of Ir(ppy)$_3$ molecules dispersed in the PS matrix with density N'_G, and L' is the thickness of the sample. Eq. 8 is similar to Eq. 6, except that photons get absorbed by the guest and energy transfer does not occur in this case. Combining Eqs. 6-8 and eliminating χ leads to the following expression:

$$<\eta_{ET}(I_0)>=\frac{Q(N'_G)}{Q(N_G)}\left(\frac{PL_{PH}(I_0)}{1-\exp-\alpha_H L}\right)\left(\frac{1-\exp-\alpha'_G L'}{PL'_{PH}(I_0)}\right) \tag{9}$$

This expression enables us to extract the total energy transfer efficiency from the experiments carried-out in films with different host and guest compositions, and for different excitation conditions. To complete the experimental evaluation of $<\eta_{ET}(I_0)>$ we have to know the quenching factor Q at different concentrations of Ir(ppy)$_3$ so that we can calculate the ratio of Q corresponding to the reference sample (with concentration N'_G) and the corresponding value of Q for the tested sample with a given concentration N_G. Fig. 3 shows the concentration quenching dependence from which the values of $Q(N'_G)$ and $Q(N_G)$ are obtained. We point out that both the concentration quenching factor Q and the transient phosphorescence lifetimes were independent on excitation in the range of energies we used in our experiments. It follows then that although our studies do not provide enough information about the exact physical mechanism that leads to the trend of Q, the quenching of phosphorescence is only due to the net concentration of guest molecules independently of the density of triplet-states.

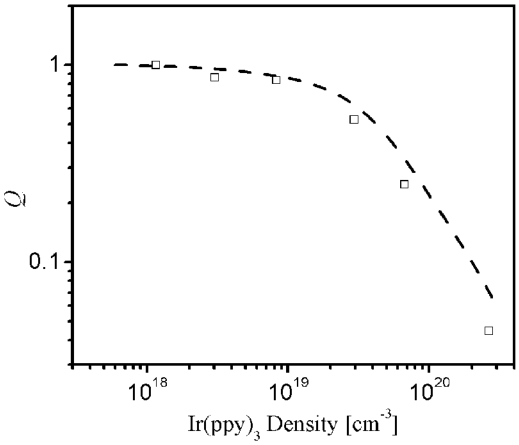

Figure 3. Quenching factor Q of the photoluminescence of Ir(ppy)$_3$ as a function of molecular density measured in PS:Ir(ppy)$_3$ films.

By using Eq. 9 the experimental value of $<\eta_{ET}(I_0)>$ was determined for the samples we prepared, while a theoretical fit was calculated from Eq. 5 using the Förster radius R_0 as the only fitting parameter. Fig. 4 shows the total energy transfer efficiency as a function of excitation I_0 for a sample with small concentrations of host and guest molecules (8 and 0.2 wt. %, respectively). The best fit to the experimental data was obtained with a radius of $R_0 = 3$ nm.

To benchmark our model, we repeated the same calculations for a variety of samples with host concentrations ranging from 0.3 up to 65 wt. % and guest concentrations ranging from 0.04 up to 5 wt. %. This time, no fitting parameter was varied and a Förster radius of 3 nm was kept constant. As shown in Fig. 5, a good agreement was found between theory and experiment.

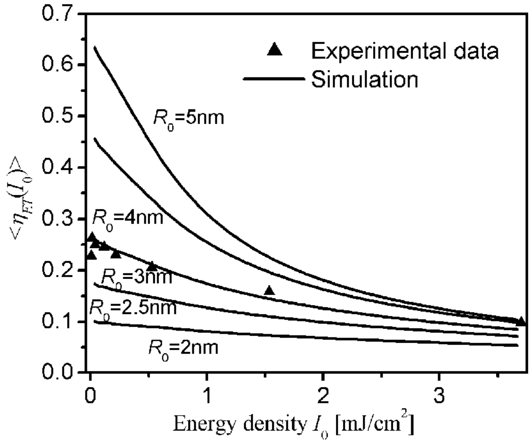

Figure 4. Total energy transfer efficiency for a thin film with composition PS:CBP:Ir(ppy)$_3$ for different excitation conditions. This film has a host and guest density of $N_H = 1\times10^{20}$ cm^{-3} and $N_G = 1.8\times10^{18}$ cm^{-3} respectively and thickness of 1.0 μm.

From the trends of $<\eta_{ET}(I_0)>$ in Fig. 5 it follows that at high concentration, the interaction range R between G-H^* tends to be smaller on average than the value of the Förster radius R_0, resulting in high values of $<\eta_{ET}(I_0)>$. For example, for a film with the structure PS:CBP:Ir(ppy)$_3$ and composition 30:65:5 wt.%, the total energy transfer efficiency is practically unity and only drops at high excitations, where the guest sites are saturated and then the host excited-states decay through other channels. In contrast, very small molecular densities increase the molecular interaction distance R and its dispersion around a central value which in turn leads to a reduction of energy transfer. Note that the value of $R_0 = 3$ nm obtained in this study is substantially different from the value of 3.8 nm obtained from the simple calculation of the overlap integral[4] between the host emission spectrum and the molar extinction coefficient for the guest, shown in Fig. 1, assuming a fluorescent quantum yield for CBP of 0.5.[15]

Having determined the Förster radius in samples with composition PS:CBP:Ir(ppy)$_3$, we can extend our numerical calculations to films with composition CBP:Ir(ppy)$_3$ (no matrix used) and predict the optimum doping concentration that gives the maximum internal quantum efficiency in such films defined as $\rho = <\eta_{ET}(I_0)>\eta_{PL}(N_G)$. Then, we first calculate the predicted total energy transfer efficiency as a function of the doping concentration N_G, for various excited host concentrations (assuming N_{H^*} is homogenous in all the volume of the film); second, we consider a phosphorescence quantum yield[16] of $\eta_{PL}(N_{G0}) = 0.4$ and the values of the quenching factor $Q(N_G)$ of Fig 3. Fig. 6 shows the so calculated values of internal quantum efficiency, where we see that the optimum guest concentration is 2.2 (wt. %) for an excited host density of 3×10^{18} cm^{-3}, but it increases up to 6.5 (wt. %) for an excited host density of 1×10^{20} cm^{-3}.

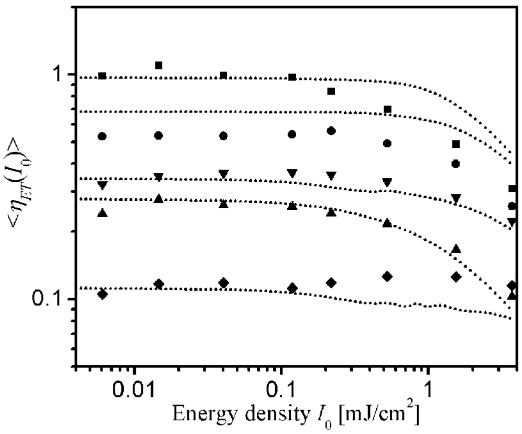

Figure 5. Experimental data and numerical simulations of total energy transfer efficiency as a function of excitation I_0 for samples with different combinations of N_H and N_G. All the simulations (dotted lines) were obtained with R_0 = 3 nm. The relative proportions of host and guest molecules were chosen in such a way that diverse interaction ranges R_j take place. (Squares) N_H = 8.1×10^{20} cm^{-3} and N_G = 4.6×10^{19} cm^{-3} [65:5 wt. %], (circles) N_H = 1.0×10^{20} cm^{-3} and N_G = 1.0×10^{19} cm^{-3} [8.1:1.1 wt. %], (up-triangles) N_H = 1.0×10^{20} cm^{-3} and N_G = 1.8×10^{18} cm^{-3} [8.1:0.2 wt. %], (down-triangles) N_H = 2.0×10^{19} cm^{-3} and N_G = 1.8×10^{18} cm^{-3} [1.6:0.2 wt. %], (diamonds) N_H = 3.7×10^{18} cm^{-3} and N_G = 3.7×10^{17} cm^{-3} [0.3:0.04 wt. %]. The thicknesses of the films are 0.3 μm, 0.9 μm, 1.0 μm, 1.1 μm and 2.3 μm respectively.

The numerical simulations depicted in Fig. 6 also show that the overall phosphorescence is strongly reduced by quenching effects and that the photoluminescence quantum yield $\eta_{PL}(N_G)$ imposes an upper limit of ρ = 0.4 for an optically-pumped film provided that the efficiency of the energy transfer process is unity. This contrasts with the high internal quantum efficiencies obtained for some electrically pumped Ir(ppy)$_3$-doped devices in which external efficiencies of 15% could be demonstrated,[17-18] corresponding to internal efficiencies as high as 75% if one assumes that only 20% of the light is coupled out of the device. From the discrepancy between electroluminescence and photoluminescence we can conclude that the upper limit of ρ = 0.4 can be attributed to a limited low intersystem crossing efficiency within the Ir(ppy)$_3$ and that the phosphorescence efficiency of the transition between the triplet excited state and the ground state in Ir(ppy)$_3$ is nearly unity. This is the case because in photoluminescence experiments, the energy is transferred from a singlet excited-state in the host to a singlet state in the guest, which in turn is transferred, by intersystem crossing, to a triplet excited-state. In contrast, in electroluminescence the transfer of energy between the host and guest can also occur through Dexter transfer.

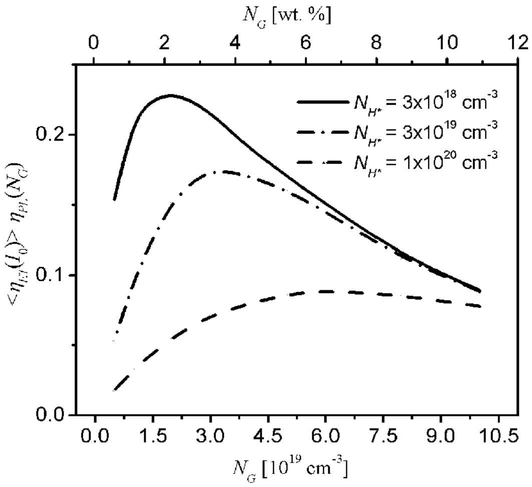

Figure 6. Internal quantum efficiency ρ calculated for a CBP:Ir(ppy)$_3$ film as a function of doping concentration N_G for different values of N_{H*}.

Conclusion

In conclusion, by measuring the integrated photoluminescence from optically pumped phosphorescent thin films and by comparing these results with those obtained from a numerical model we could extract a Förster radius of 3 nm for the system CBP:Ir(ppy)$_3$. The numerical model we developed to describe this process accounted for the inhomogeneous excitation in the sample and was corrected for quenching effects between the excited guest molecules. A good agreement between experiment and calculations was found using as only fitting parameter the Förster radius. Our results show that for Ir(ppy)$_3$ concentrations above 10^{19} cm^{-3} quenching reduces the phosphorescence efficiency. When Förster energy transfer in these films is optimized, the overall efficiency of phosphorescence reaches 0.4 and is mainly limited by the efficiency for intersystem crossing in Ir(ppy)$_3$. These studies confirm that in electrophosphorescent devices based on Ir(ppy)$_3$ light emission resulting from the formation of singlet excited states in the host and their transfer through a Förster process is negligible compared with the formation of either triplets directly formed from injected charges or triplets that are formed through a Dexter energy transfer from triplets of the host.

Acknowledgments

This work was funded by NSF through a CAREER grant, by ONR, by NASA through The University of Alabama at Huntsville and by funds through the Arizona State Prop. 301. G. R.-O. acknowledges support from the Mexican governmental agency CONACYT.

References

1. C. W. Tang, S. A. VanSlyke, C. H. Chen, *J. Appl. Phys*., **65**, 3610 (1989), **65**, 3610.
2. C. W. Tang, D. J. Williams, and J. C. Chang, US Patent # 5,294,870 (1994).
3. M. Berggren, A. Dodabalapur, R. E. Slusher, Z. Bao, *Nature*, **389**, 466 (1997).
4. N. J. Turro, *Modern Molecular Photochemistry* (Benjamin-Cummings, Menlo Park, 1978).
5. S. Hoshino and H. Suzuki, Appl. Phys. Lett., **69**, 224 (1996).
6. M. A. Baldo, D. F. O'Brien, Y. You, A. Shoustikov, S. Sibley, M. E. Thompson, S. R. Forrest, *Nature*, **395**, 151 (1998).
7. M. A. Baldo, S. Lamansky, P. E. Burrows, M. E. Thompson, S. R. Forrest, *Appl. Phys. Lett*., **75**, 4 (1999).
8. M. A. Baldo, M. E. Thompson, S. R. Forrest, *Nature*, **403**, 750 (2000).
9. M. A. Baldo, S. R. Forrest, *Phys. Rev. B*, **62**, 10958 (2000). M. A. Baldo, Adachi, S. R. Forrest, *Phys. Rev. B*, **62**, 10967 (2000)
10. T. Virgili, D. G. Lidzey, D. D. C. Bradley, *Synthetic Metals*, **111-112**, 203 (2000).
11. G. Cerullo, S. Stagira, M. Zavelani-Ross, S. De Silvestri, T. Virgili, D. G. Lidzey, D. D. C. Bradley, *Chem. Phys. Lett*., **335**, 27 (2201).
12. A. Dogariu, R. Gupta, A. J. Heeger, H. Wang, *Synthetic Metals,* **100**, 95 (1999).
13. G. Cerullo, M. Nisoli, S. Stagira, S. De Silvestri, G. Lanzani, W. Graupner, E. List, G. Leising, *Chem. Phys. Lett*., **288**, 561 (1998).
14. A. R. Buckley, M. D. Rahn, J. Hill, J. Cabanillas-Gonzalez, A. M. Fox, D. D. C. Bradley, *Chem. Phys. Lett*., **339**, 331 (2001).
15. V. G. Kozlov, G. Parthasarathy, P. E. Burrows, S. R. Forrest, Y. You, M. E. Thompson, *Appl. Phys. Lett*., **72**, 144 (1998).
16. K. A. King, P. J. Spellane, R. J. Watts, *J. Am. Chem. Soc.*, **107**, 1431 (1985).
17. T. Watanabe, K. Nakamura, S. Kawami, Y. Fukuda, T. Tsuji, T. Wakimoto, S. Miyaguchi, *SPIE*, **4105**, 175 (2000).
18. C. Adachi, M. A. Baldo, S. R. Forrest, M. E. Thompson, *Appl. Phys. Lett*., **77**, 904 (2000).

Biography

Gabriel Ramos-Ortiz received his B.S. degree in Physics from the National Autonomous University of Mexico in 1996. Since 1998 he has been part, as PhD student, of the *Polymer and Molecular electronics Group* directed by Dr. Bernard Kippelen at the Optical Sciences Center, University of Arizona. His work focuses on basic properties of emissive molecules used in electroluminescent devices, optical amplification and laser action as well as nonlinear optical activity in organic materials.